metals

Article

Effect of Auto-Tuning on Serrated Flow Behavior

S.M.A.K. Mohammed and D.L. Chen *

Department of Mechanical and Industrial Engineering, Ryerson University, Toronto, ON M5B 2K3, Canada
* Correspondence: dchen@ryerson.ca; Tel.: +1-416-979-5000 (ext. 6487); Fax: +1-416-979-5265

Received: 22 July 2019; Accepted: 27 July 2019; Published: 31 July 2019

Abstract: The mechanical response of a servo-hydraulic testing system is affected by the stiffness of test specimens. An adaptive controller helps in auto-tuning the system by setting the optimal proportional-integral-derivative values for the subsequent test as the stiffness changes. This paper presents the effect of auto-tuning of various channels on the flow response of several commercial Al and Mg alloys and a mild steel. Strain-controlled monotonic tensile tests were performed at a given strain rate of 1×10^{-4} s^{-1} after auto-tuning of position, load, and strain channels in different combinations. Serrated flow or Portevin–Le Chatelier effect was observed in the Al alloys after auto-tuning of either position channel only or position and load channels. However, the serrations of Al alloys were shielded after further auto-tuning of strain channel. The stress-strain curves of Mg alloys and mild steel were observed to be basically free of serrations under any combinations of auto-tuning, which confirms that the serrated flow is a property of specific materials rather than a machine system noise.

Keywords: auto-tuning; strain control; Portevin–Le Chatelier effect; serrated flow

1. Introduction

Excessive oscillatory tendency in the hydraulic systems is the primary cause for instability of the system. The performance is affected by the PID (proportional-integral-derivative) control parameters based on the stiffness of specimens. Most of the mechanical tests are conducted under load or strain control mode. As the specimen stiffness decreases, the bandwidth tends to reduce under load control, making the response sluggish. In contrast, the gain increases with decreasing stiffness under strain control mode, leading to an unstable loop system [1]. In the past, the oscillations were misinterpreted as mere machine noise rather than a material property [2]. It was reported that the oscillations/serrations observed during load-controlled tests were due to the sluggish response of a material. However, under strain-controlled tests, the machine becomes unstable and generates noise if tuning was not properly performed [1,2]. With the advancement in the controller design, engineers started using automatic tuning of the machine rather than manual tuning [3,4]. The process of automatic tuning of PID control parameters is known as auto-tuning. Sometimes, the stiffness of a sample changes during testing because of crack propagation or transition from linear elastic to plastic behavior. Thus, the machine needs to be auto-tuned to compensate the gain and lag of the controller [2,5,6]. Hence, auto-tuning became a necessity rather than an option in the contemporary fatigue testing machine.

Typically, in a servo-hydraulic system, there are three sensors, i.e., linear variable differential transformer (LVDT), load cell, and extensometer which needs to be tuned as the stiffness or type of test materials changes. The process of auto-tuning of a certain channel is served to accomplish the test with accurate results and control performance. Although the system was being stable during the tests, many researchers have reported the serrated flow in some materials under a certain strain rate and temperature range [7–11]. It was considered as the material property rather than the noise of machine system, commonly referred to as the Portevin-Le Chatelier (PLC) effect in numerous papers and books, e.g., [12–19].

The serrated flow phenomenon or PLC effect, which is common in some structural materials such as aluminum and steel, causes localized deformation which in turn becomes the ground to structural issues. The associated localized deformation increases the flow stress, ultimate tensile strength (UTS), and work hardening rate at the expense of ductility and fracture toughness. Serrated flow reflects the dynamic properties of shear bands and the underlying physics [11]. The mechanism of serrated flow has been a subject of significant interest. The plastic deformation in metals and alloys is mainly attributed to the nucleation and motion of dislocations [20]. The PLC effect has been investigated by stress and strain-controlled tensile tests as well as digital image correlation and acoustic emission [21]. Recently some researchers have reported the PLC effect under compressive loading as well [9].

In the present study, we reported for the first time, the effect of auto-tuning of various channels of a hydraulic fatigue testing system on the mechanical response of materials. The effect of auto-tuning of strain channel under strain control mode is of particular interest of the present study.

2. Materials and Methods

Monotonic tensile tests were conducted at room temperature under strain control mode at a constant strain rate of 1×10^{-4} s^{-1} to a fixed strain of 2% after auto-tuning of different channels in an Instron 8801 servo-hydraulic fatigue testing system of a capacity of 50 kN. In the initial testing, auto-tuning of only position channel (P) was performed followed by the tensile test under strain control mode. In the second scenario, auto-tuning of position and load channels (P + L) was performed followed by the tensile test of the same sample until 2% strain. Finally, in the last scenario, auto-tuning of all the three channels, i.e., position, load, and strain channels (P + L + S), was performed followed by the tensile test at the same strain rate to a strain of 2% as well. The tensile tests were carried out on several materials including aluminum alloys (AA6061-T621, AA2024-T3), magnesium alloys (ME20-H112, ZK60), and a mild steel specimen. The details of fabrication of AA6061-T621 [22], AA2024-T3 [23], and magnesium ME20-H112 [24] can be found elsewhere.

3. Results and Discussion

3.1. The Effect of Auto-Tuning

The change in the stiffness of test specimens affects the natural frequency and damping. Thus, testing a new specimen demands tuning using adaptive controller. The adaptive controller is required to maintain the performance, irrespective of the specimen type or specimens with varying stiffness values. Three-term PID control of a system shown in Figure 1 is generally used in the interacting form, which can be expressed as follows [25]:

$$C(s) = \frac{u(t)}{e(t)} = G_c \frac{(1 + sT_i)(1 + sT_d)}{st_i}, \tag{1}$$

where $C(s)$ is controller function, $u(t)$ is the control action, $e(t)$ is the error, T_i and T_d are integral and derivative times, respectively. The signal $u(t)$ controls the servo-valve, which in turn regulates the flow of oil into and out of the actuator [25].

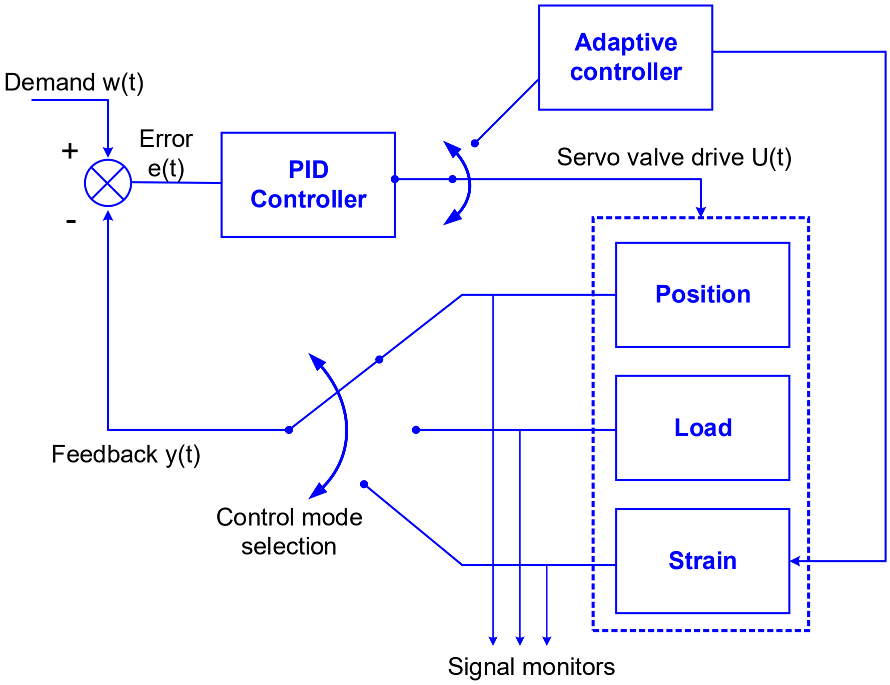

Figure 1. Control system of position, load, and strain channels under a strain control mode.

The purpose of auto-tuning is to optimize its own internal running parameters so as to maximize or minimize the fulfilment of an objective function—typically, the maximization of efficiency or the minimization of error. The main objective of auto-tuning the strain channel is to minimize the oscillations under strain control mode.

In a control system, self-tuning is usually composed of four components:

i expectations (here we treat it as the defined strain rate),
ii measurement (the system measures the strain rate),
iii analysis (the control system compares the defined rate with the measured rate), and
iv actions (the system uses PID or other method to minimize the discrepancy).

During auto-tuning of strain channel, it is expected that the system compensates the relaxation of test materials and tends to pull the specimen at the defined strain rate under strain control mode. For instance, in the low cycle fatigue (LCF) tests, the oscillations may appear when the extension is increasing if the system becomes unstable. Clarke and Hinton [2] pointed out that these oscillations may be misinterpreted as special material characteristics. However, several researchers have observed and concluded that the serration phenomenon is actually a material property and it depends on the material type, strain rate and temperature [7,10–12,15,21,26,27]. Nevertheless, the effect of auto-tuning on the serration behavior has not been reported so far. To determine more accurately the material behavior, it is necessary to identify the effect of auto-tuning on the material properties.

3.2. Mechanism of Serrated Flow Behavior

The tensile stress-strain results of various alloys conducted after different combinations of auto-tuning of position, load, and strain are presented in Figure 2a–c, respectively. It is evident that the serrations were observed only in the aluminum alloys in both cases of position (P) auto-tuning only (Figure 2a) and position and load (P + L) auto-tuning (Figure 2b). In contrast, the stress-strain curves of magnesium alloys and mild steel specimens were found to be basically smooth in the absence of stress drops. The stress drop in carbon steel specimens are usually observed during the test, once the specimen begins to yield [1], normally called the yield-point phenomenon. This is due to the fact that there is an abrupt transition from elastic state to elastic-plastic state [28,29]. Interestingly, the serrations were absent in all of the tested materials including aluminum samples after further auto-tuning of strain channel (i.e., P + L + S), as can be seen from Figure 2c. Such an effect of auto-tuning on the tensile stress–strain curves obtained from a servo-hydraulic fatigue testing system has not been reported, to the best of the authors' knowledge. After the auto-tuning of strain channel, the stress drops are treated by the system as noise under strain control. Due to the change in stiffness of the specimen, the response becomes sluggish under load control, whereas instability under strain control occurs due to the increase in closed-loop gain [2]. Thus, the controlling system makes an effort to filter out the serrations after auto-tuning of strain channel to maintain the stabilization under strain control. Regardless of material types/characteristics or loading conditions, the serrations/oscillations are being smoothened after strain channel auto-tuning. Thus, several designers have suggested the use of adaptive controller rather than manual tuning in order to cope with the problem of variability among different specimens. Moreover, the lack of control-specific expertise of typical users of servo-hydraulic fatigue testing systems will be minimized with the use of auto-tuning by adaptive controller. The Young's modulus of the alloys was also calculated from the tensile stress-strain results and obtained to be 208, 74, 72, 40 and 46 GPa for mild steel, AA6061-T621, AA2024-T3, ME20-H112, and ZK60, respectively.

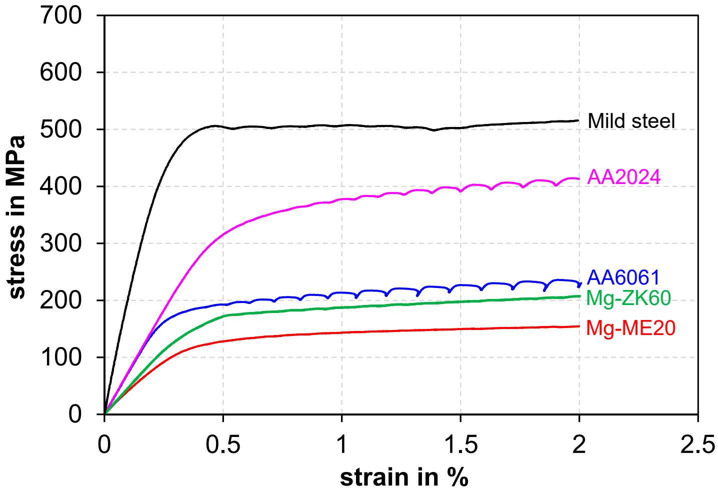

(a)

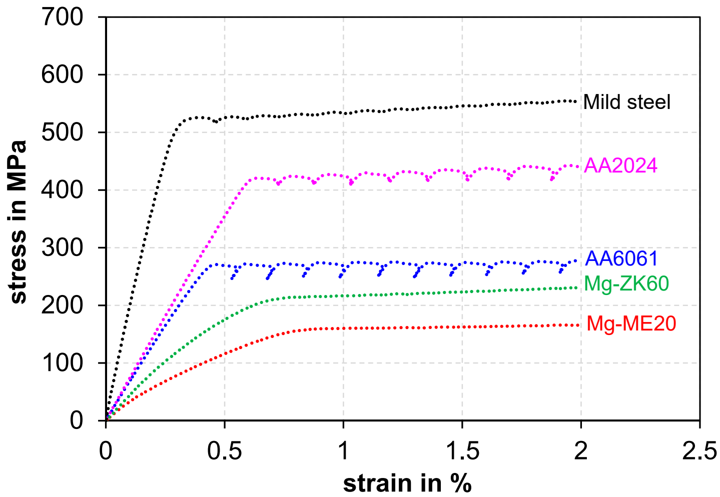

(b)

Figure 2. *Cont.*

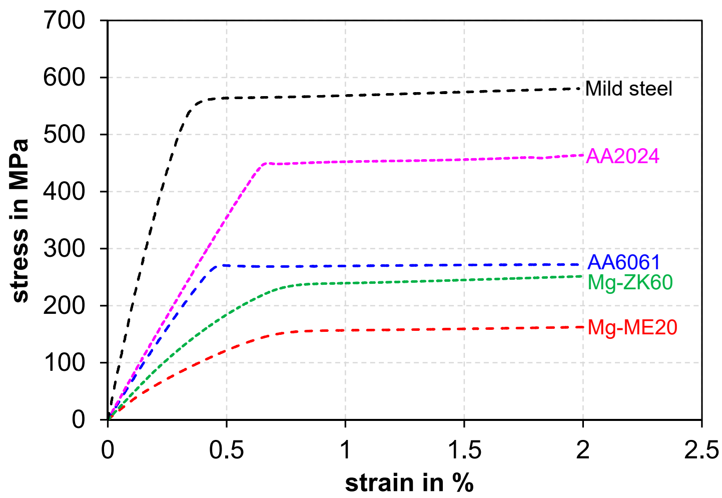

(c)

Figure 2. Tensile stress-strain curves after (**a**) position (P) auto-tuning, (**b**) position and load (P + L) auto-tuning, and (**c**) position, load, and strain (P + L + S) auto-tuning.

To confirm the presence of serrations, we have tested magnesium and steel specimens under the same test conditions for aluminum alloys. However, no serrations were observed in both magnesium (ZK60 and ME20) and mild steel specimens under the present three combinations of auto-tuning, as seen from Figure 2a–c. The yield stress of AA6061 and AA2024 alloy was obtained to be higher than that of the magnesium alloys and lower than that of the steel. This suggests that the serrations are not related to the strength level rather a property of specific materials.

The strain beyond which serrations were observed is known as a critical strain (ε_c). The critical strain for the serration increases with increasing strain rate exponentially. This is an indication of pseudo-PLC effect [27]. It is reported that the critical strain induced by dynamic strain ageing (DSA) is proportional to the strain rate and inversely proportional to the temperature [8,26]. The critical strain has been considered as an important parameter in modeling DSA behavior [15,30,31]. The models assumed that the solute atoms interact with mobile dislocations. In the presence of dislocation pile-ups in a solute atmosphere, locking and unlocking of dislocations lead to serrations. The critical strain for the onset of a serration can be expressed as [7,10]:

$$\varepsilon_c^{(m+\beta)} = K\dot{\varepsilon}\exp(Q/RT), \tag{2}$$

where m and β are the strain components arising from the vacancy concentration C_v and mobile dislocation density ρ_m during plastic deformation, respectively, K is a constant, Q is the activation energy for the serrated flow, R is the gas constant, and T is the absolute temperature. A typical value of $m + \beta$ lies in-between 2–3 for substitutional solid solution alloys, whereas it lies in-between 0.5–1 for interstitial solid solution alloys [7,10]. It is well known that the total strain is a combination of elastic and plastic strain ($\varepsilon = \varepsilon_e + \varepsilon_p$). From Hooke's law, $\sigma \propto \varepsilon_e$:

$$\dot{\varepsilon} = \dot{\varepsilon}_e + \dot{\varepsilon}_p, \tag{3}$$

$$\dot{\varepsilon} = \left[\frac{d\sigma/dt}{E_s}\right] + \dot{\varepsilon}_p, \tag{4}$$

where $\dot{\varepsilon}$, $\dot{\varepsilon}_e$, and $\dot{\varepsilon}_p$ are total, elastic and plastic strain rates, respectively. E_s is the Young's modulus of the test specimen. The stress rate, $\dot{\sigma}$, which is defined as the change in stress ($\Delta\sigma = \sigma_2 - \sigma_1$) with respect to time, is negative when the change in stress is negative. This is possible only when $\dot{\varepsilon}_p > \dot{\varepsilon}$. Thus, a load drop or serration appears when the plastic strain rate is higher than the imposed strain rate. This suggests that plastic flow becomes inhomogeneous, leading to the formation of a band (referred to as PLC band) which continues to propagate.

Typical curves of stress and displacement with respect to time of AA6061 and Mg-ME20 alloys after load and position auto-tuning is plotted in Figure 3a,b, respectively. It is obvious that the displacement–time (*d*–*t*) curve of AA6061 is step-like and the stress–time (σ–*t*) curve represents the corresponding oscillations in Figure 3a. Similar behavior was reported by Qian et al. [10] in a twinning-induced plasticity steel at different strain rates. Apparently, the onset of serrations coincides with an abrupt change of the crosshead displacement. The localized high strain in the bands inside of the gage length is the characteristics for the nucleation of serrations [7,32]. In the case of AA6061 alloy, the abrupt increase in the stress coincides with an increase in the crosshead displacement, while the halt (or slight decrease) in the displacement corresponds to a decrease in the stress (Figure 3a). In contrast, Figure 3b represents a smooth and linearly increasing curve of displacement vs. time, confirming the smooth flow curve free of oscillations in the ME20 magnesium alloy in Figure 2b, although the stress vs. time curve exhibits some extent of noise but it looks pretty much linear without the nearly periodic oscillations in the AA6061 aluminum alloy in Figure 3a. The different trends in Figure 3a,b would further confirm that the stress drops/serrations are related to specific material characteristics rather than the machine noise.

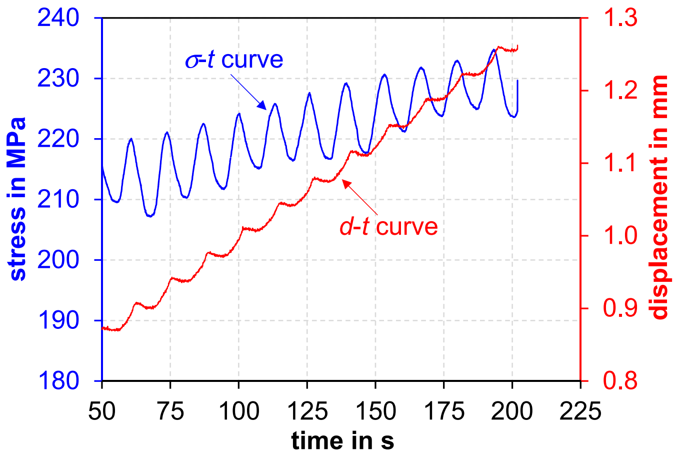

(**a**)

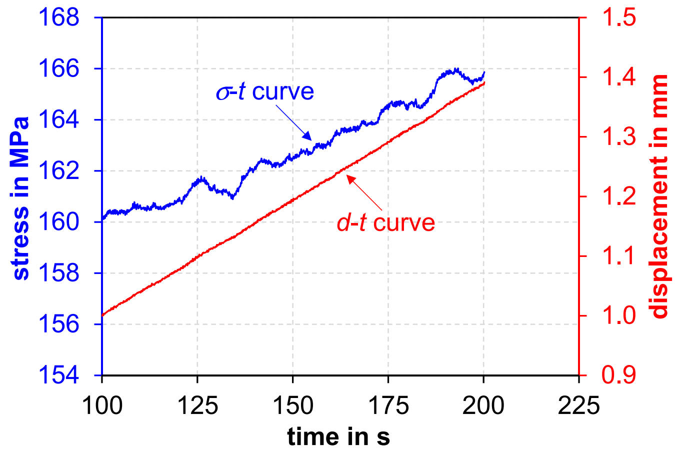

(**b**)

Figure 3. Typical stress and displacement versus time curves of (**a**) AA6061 and (**b**) Mg-ME20 alloy under a strain control mode, obtained after position and load (P + L) auto-tuning.

Figure 4 presents the load vs. time curves of two typical Al (6061) and Mg (ME20) alloys. It can be seen that the AA6061 alloy presents oscillation-like curve after yielding in both auto-tuning cases of position channel and position and load channels, while the oscillations/serrations are basically absent after auto-tuning of all three channels of position, load and strain. This is in sharp contrast with the situation of ME20 magnesium alloy tested in the identical conditions/parameters as those for AA6061 alloy, where oscillations/serrations are also absent in such load vs. time curves in all of the three auto-tuning cases (P, P + L, and P + L + S). Due to the interaction of mobile dislocations and solute atoms or nano-sized precipitates in the Al alloy during deformation, the stress or load drop at a constant strain rate is reflected on the crosshead displacement with respect to time. The different characteristics exhibited by the aluminum alloy and magnesium alloy shown in Figure 4, determined using the identical experimental parameters/conditions, would provide corroboration that the serrations are actually a material property as commonly referred to as the PLC effect, rather than the machine system noise.

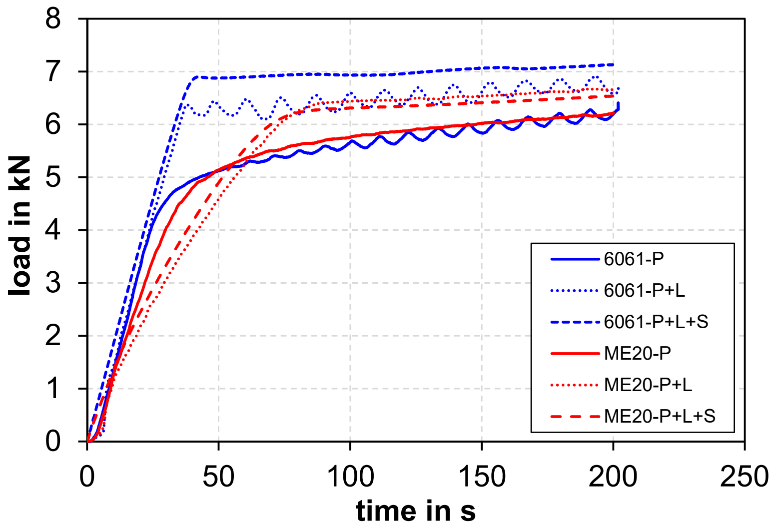

Figure 4. Load vs. time curves of AA6061 and ME20 alloys obtained after various combinations of auto-tuning.

4. Conclusions

The effect of auto-tuning in different cases on the serrated flow behavior of materials has been explored. The following conclusions could be drawn:

(1) The auto-tuning by adaptive controller is an effective way for the controlling performance of servo-hydraulic fatigue testing machine. However, the auto-tuning of strain channel after the auto-tuning of position and load channels would shield the real material characteristics under strain control mode due to the self-adjustment set by the optimized PID values via adaptive controller.

(2) The serrations are related to the real material property, depending on the material type, strain rate, and temperature. The serrations in the aluminum alloy are observed at room temperature after auto-tuning of either position channel only or position and load channels. In sharp contrast, no serrations are observed in the magnesium alloy and mild steel samples after auto-tuning of any channel.

Author Contributions: Conceptualization, S.M.A.K.M. and D.L.C.; methodology, S.M.A.K.M. and D.L.C.; investigations, S.M.A.K.M.; formal analysis, S.M.A.K.M. and D.L.C.; data curation, S.M.A.K.M.; writing—original draft preparation, S.M.A.K.M.; writing—review and editing, S.M.A.K.M. and D.L.C.; supervision, D.L.C.

Funding: This research was funded by the Natural Sciences and Engineering Research Council of Canada (NSERC).

Acknowledgments: The authors would like to thank Chao Ma for fruitful discussion throughout the work and Qiang Li, Alan Machin, Joseph Amankrah, and Roy Churaman for easy access to the laboratory facilities of Ryerson University and their assistance in the experiments.

Conflicts of Interest: The authors declare no conflict of interest. The funders had no role in the design of the study; in the collection, analyses, or interpretation of data; in the writing of the manuscript, or in the decision to publish the results.

References

1. Hinton, C. Adaptive PID control of dynamic materials-testing machines using remembered stiffness. In *Applications of Automation Technology to Fatigue and Fracture Testing and Analysis*; ASTM International: West Conshohocken, PA, USA, 1997; pp. 111–119.
2. Clarke, D.W.; Hinton, C.J. Adaptive control of materials-testing machines. *Automatica* **1997**, *33*, 1119–1131. [CrossRef]
3. Nishikawa, Y.; Sannomiya, N.; Ohta, T.; Tanaka, H. A method for auto-tuning of PID control parameters. *Automatica* **1984**, *20*, 321–332. [CrossRef]
4. Kasprzyczak, L.; Macha, E. Selection of settings of the PID controller by automatic tuning at the control system of the hydraulic fatigue stand. *Mech. Syst. Signal Process.* **2008**, *22*, 1274–1288. [CrossRef]
5. Liu, G.P.; Daley, S. Optimal-tuning nonlinear PID control of hydraulic systems. *Control Eng. Pract.* **2000**, *8*, 1045–1053. [CrossRef]
6. Elbayomy, K.M.; Zongxia, J.; Huaqing, Z. PID Controller Optimization by GA and Its Performances on the Electro-hydraulic Servo Control System. *Chin. J. Aeronaut.* **2008**, *21*, 378–384. [CrossRef]
7. Rodriguez, P. Serrated plastic flow. *Bull. Mater. Sci.* **1984**, *6*, 653–663. [CrossRef]
8. Nakada, Y.; Keh, A. Serrated flow in Ni-C alloys. *Acta Metall.* **1970**, *18*, 437–443. [CrossRef]
9. Pozuelo, M.; Chang, Y.W.; Marian, J.; Yang, J.M. Serrated flow in nanostructured binary Mg-Al alloys. *Scr. Mater.* **2017**, *127*, 178–181. [CrossRef]
10. Qian, L.; Guo, P.; Zhang, F.; Meng, J.; Zhang, M. Abnormal room temperature serrated flow and strain rate dependence of critical strain of a Fe–Mn–C twin-induced plasticity steel. *Mater. Sci. Eng. A* **2013**, *561*, 266–269. [CrossRef]
11. Fan, Z.; Li, Q.; Fan, C.; Wang, H.; Zhang, X. Strategies to tailor serrated flows in metallic glasses. *J. Mater. Res.* **2019**, 1–13. [CrossRef]
12. Yilmaz, A. The Portevin–Le Chatelier effect: A review of experimental findings. *Sci. Technol. Adv. Mater.* **2011**, *12*, 063001. [CrossRef] [PubMed]
13. Halim, H.; Wilkinson, D.; Niewczas, M. The Portevin–Le Chatelier (PLC) effect and shear band formation in an AA5754 alloy. *Acta Mater.* **2007**, *55*, 4151–4160. [CrossRef]
14. Jiang, H.; Zhang, Q.; Chen, X.; Chen, Z.; Jiang, Z.; Wu, X.; Fan, J. Three types of Portevin–Le Chatelier effects: Experiment and modelling. *Acta Mater.* **2007**, *55*, 2219–2228. [CrossRef]
15. McCormigk, P. A model for the Portevin-Le Chatelier effect in substitutional alloys. *Acta Metall.* **1972**, *20*, 351–354. [CrossRef]
16. Cottrell, A.H. LXXXVI. A note on the Portevin-Le Chatelier effect. *Lond. Edinb. Dublin Philos. Mag. J. Sci.* **1953**, *44*, 829–832. [CrossRef]
17. Penning, P. Mathematics of the portevin-le chatelier effect. *Acta Metall.* **1972**, *20*, 1169–1175. [CrossRef]
18. Kubin, L.P.; Estrin, Y. Evolution of dislocation densities and the critical conditions for the Portevin-Le Châtelier effect. *Acta Metall. Mater.* **1990**, *38*, 697–708. [CrossRef]
19. McCormick, P. The Portevin-Le Chatelier effect in an Al-Mg-Si alloy. *Acta Metall.* **1971**, *19*, 463–471. [CrossRef]
20. Cottrell, A.H. *Dislocations and Plastic Flow in Crystals*; Clarendon Press: Oxford, MS, USA, 1953.
21. Härtel, M.; Illgen, C.; Frint, P.; Wagner, M. On the PLC effect in a particle reinforced AA2017 alloy. *Metals* **2018**, *8*, 88. [CrossRef]
22. Feng, A.H.; Chen, D.L.; Ma, Z.Y. Microstructure and cyclic deformation behavior of a friction-stir-welded 7075 Al alloy. *Metall. Mater. Trans. A* **2010**, *41*, 957–971. [CrossRef]
23. Niu, P.L.; Li, W.Y.; Li, N.; Xu, Y.X.; Chen, D.L. Exfoliation corrosion of friction stir welded dissimilar 2024-to-7075 aluminum alloys. *Mater. Charact.* **2019**, *147*, 93–100. [CrossRef]

24. Mirza, F.A.; Wang, K.; Bhole, S.D.; Friedman, J.; Chen, D.L.; Ni, D.R.; Xiao, B.L.; Ma, Z.Y. Strain-controlled low cycle fatigue properties of a rare-earth containing ME20 magnesium alloy. *Mater. Sci. Eng. A* **2016**, *661*, 115–125. [CrossRef]
25. Clarke, D.W. PID algorithms and their computer implementation. *Trans. Inst. Meas. Control* **1984**, *6*, 305–316. [CrossRef]
26. Lee, S.Y.; Hwang, B. Dynamic strain aging and serration behavior of three high-manganese austenitic steels. *Metall. Mater. Trans. A* **2019**. [CrossRef]
27. Rai, R.K.; Sahu, J.K. Mechanism of serrated flow in a cast nickel base superalloy. *Mater. Lett.* **2018**, *210*, 298–300. [CrossRef]
28. Schwab, R.; Ruff, V. On the nature of the yield point phenomenon. *Acta Mater.* **2013**, *61*, 1798–1808. [CrossRef]
29. Brindley, B.J.; Worthington, P.J. Yield-point phenomena in substitutional alloys. *Metall. Rev.* **1970**, *15*, 101–114.
30. Van Liempt, P.; Onink, M.; Bodin, A. Modelling the influence of dynamic strain ageing on deformation behaviour. *Adv. Eng. Mater.* **2002**, *4*, 225–232. [CrossRef]
31. Rizzi, E.; Hähner, P. On the Portevin–Le Chatelier effect. *Int. J. Plast.* **2004**, *20*, 121–165. [CrossRef]
32. Lebedkina, T.A.; Lebyodkin, M.A.; Chateau, J.-P.; Jacques, A.; Allain, S. On the mechanism of unstable plastic flow in an austenitic FeMnC TWIP steel. *Mater. Sci. Eng. A* **2009**, *519*, 147–154. [CrossRef]